

A numerical study on strengthening GFRP-reinforced concrete one-way slabs with openings using CFRP sheets

Ngoc Tan Nguyen⁽¹⁾, Anh Dung Tran⁽²⁾, Van Trong Vu⁽³⁾



Abstract

Openings in concrete slabs offer architectural benefits but require careful consideration for maintaining structural integrity. Fiber-reinforced polymer (FRP) is considered a robust solution for enhancing the durability of reinforced concrete (RC) structures in challenging conditions. FRP can serve both as reinforcement and as strengthening material to provide a sufficient structural load capacity. This paper investigates the flexural performance of one-way concrete slabs with openings reinforced by glass fiber-reinforced polymer (GFRP) bars and strengthened with carbon fiber-reinforced polymer (CFRP) sheets. Additionally, it aims to examine various factors influencing the performance of RC slabs and to evaluate the effectiveness of CFRP strengthening methods in enhancing the load-carrying capacity of slabs with openings. A parametric study using finite element analysis (FEA) is conducted, focusing on factors that influence structural capacity, including the compressive strength of concrete, GFRP reinforcement ratio, and the layout of CFRP sheets.

Key words: One-way slab, GFRP bars, CFRP sheets, Nonlinear finite element analysis

1. Introduction

Openings provide various architectural benefits for concrete slabs, such as providing lighting, enhancing air circulation, accommodating stairs and elevators, and facilitating cooling and heating ducts. While these openings are beneficial, they also weaken the concrete structure. To address this issue, various strengthening methods have been studied and developed. One of the most prevalent and widely used methods involves the use of fiber-reinforced polymer materials. Carbon fiber-reinforced polymer sheets are particularly popular thanks to their easy installation with externally bonded technique and their diversity of manufactured shapes. Thus, they are extensively used in structural engineering to reinforce and retrofit concrete buildings. Moreover, FRP materials also have better resistance in corrosive environments. This suggests their use as an alternative to traditional steel rebars used in concrete structures for centuries. In effect, in harsh environmental conditions like marine environments, steel reinforcement is highly susceptible to rapid corrosion. This can result in costly repairs, reduced service life, and even structural failure. Recent advancements in polymer technology have resulted in the development of modern FRP reinforcing bars, particularly those made of glass. GFRP bars are a non-corrosive alternative to steel reinforcement and are especially suitable for corrosive environments. Over the past decade, GFRP bars have been more commonly used as reinforcement due to their lightweight nature, ease of installation, corrosion resistance, and high tensile strength.

Numerous studies, by experiments as well as by numerical analysis, have investigated the application of FRP materials for reinforcing structural elements, especially beams and slabs, and strengthening those with openings. Naser et al. [1] presented a review of the FEA strategies of RC beams strengthened with FRP, such as element types and material parameters. Anil et al. [3] investigated the flexural behavior of RC slabs with openings, focusing on the impact of opening sizes and locations, and evaluated the effectiveness of CFRP strips for strengthening. An experimental program was carried out on thirteen specimens, comparing strength, stiffness, ductility, and energy dissipation capacities, aiming to develop an efficient and easy-to-apply strengthening technique. Afefy et al. [4] tested seven one-way slabs to investigate the impact of openings and strengthening techniques on flexural performance, with six having openings and one serving as a reference. The results showed that a hybrid strengthening technique combining near-surface mounted steel bars on the tension side and an engineered cementitious composites overlay on the compression side was most effective, restoring and enhancing the structural performance of the slabs compared to the reference one. Nguyen et al. [5] investigated the impact of several factors, such as concrete strength, reinforcement ratio, and steel-concrete bond strength, on the performance of corroded RC beams with CFRP sheets. This study concluded that CFRP sheets were effective for these structural elements with corrosion of longitudinal rebars greater than 10%, which translated into a 50% decrease in bond strength. Nguyen et al. [2] conducted a nonlinear FEA to investigate further these influencing factors on the flexural capacity of FRP-strengthened full-size RC beams. Vu et al. [6] proposed a framework for predicting the flexural behavior of beams with CFRP sheets, incorporating various parameters and failure modes, particularly premature ones like intermediate crack-induced and delamination debonding. Verified against an experimental database of 165 RC beams, this study presented effective predictions of the load-bearing capacity and failure modes of FRP-strengthened beams across different loading levels.

The purpose of this study is to use nonlinear finite element (NLFE) analysis to examine the flexural behavior of a one-way concrete slab with openings reinforced with GFRP bars and strengthened using CFRP sheets. The study has two primary

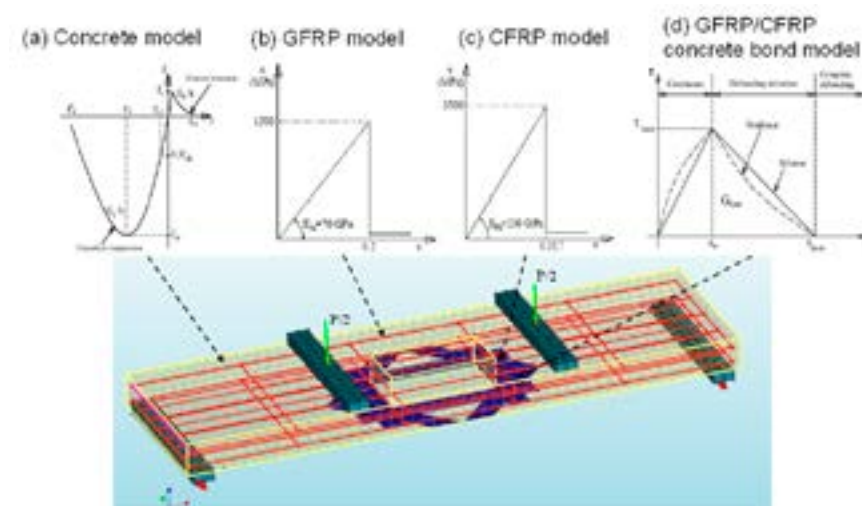


Figure 1. NLFE model of the slab sample

objectives, which will be explored through parametric investigations focusing on the compressive strength of concrete, the GFRP reinforcement ratio, and the layout of CFRP sheets. The first objective is to understand how these factors influence the maximum load, stiffness, and deformation of RC slabs reinforced with GFRP bars. The second objective is to evaluate the effectiveness of the CFRP strengthening method in enhancing the load-carrying capacity of slabs with openings.

2. Modeling of CFRP-strengthened GFRP concrete slabs

In this study, a concrete slab sample reinforced with GFRP bars and strengthened with CFRP sheets is the principal component under consideration. The sample had the same dimensions as the one studied by Golham et al. [7]. Its dimensions were 150×750×2650 mm in depth × width × length. Furthermore, the slab was modeled with a rectangular opening in the center with dimensions of 250×500 mm in width × length. The slab samples were placed on a roller and a pinned support whose center-to-center distance was 2500 mm. At the bottom layer, GFRP reinforcement comprised 8 and 6 bars in the longitudinal and transverse axes. At the top layer, GFRP reinforcement comprised 5 and 6 bars in the longitudinal and transverse axes. All GFRP bars had the same diameter of 8 mm and were placed with regular spacing between them. An NLFE model of the sample was built to investigate its behavior using DIANA software, as shown in Figure 1. Concrete was modeled through a total-strain-based rotating smeared crack model using the CHX60 elements, with mechanical behavior simulated by

stress-strain curves in compression and tension, as shown in Figure 1(a). The mesh size of the concrete was discretized with dimensions equal to 50×50×50 mm. A study was conducted to assess the mesh sensitivity. This value ranged from 20 mm to 60 mm, corresponding to three times the size of coarse aggregate with a maximal diameter of 19 mm. The results showed that the mesh element size of 50×50×50 mm achieved similar accuracy compared to that of a 20×20×20 mm mesh while significantly reducing computational time and resource requirements. The experimental slab was made of concrete with a mean compressive strength of 49.2 MPa on cylindrical samples at 28 days. Its characteristic compressive strength (f_{ck}) and the average tensile strength (f_t) were determined to be 41.2 MPa and 3.6 MPa, respectively. The modulus of elasticity (E_c) of the concrete was taken as 35 GPa. The GFRP bars were modeled as embedded bar elements within the concrete elements. Their tensile behavior was simulated by a linear stress-strain relationship, as illustrated in Figure 1(b), where their ultimate strength (f_u) was taken as 1500 MPa with a maximum strain of 20% and a modulus of elasticity (E_u) of 70 GPa. Since these GFRP bars were ribbed, an assumption of good bond was applied to describe the adhesion between the GFRP bars and the concrete.

The CFRP sheets were modeled using CQ40S elements, which are eight-node quadrilateral isotropic curved shell elements. Their mechanical behavior was represented by a linear stress-strain relationship under tensile stress, as illustrated in Figure 1(c). The detailed parameters of the CFRP sheet included thickness (t_f) of 0.167 mm, tensile strength (f_{fu}) of 3500 MPa, and modulus of elasticity (E_f) of 230 GPa. In theoretical calculations, the load-carrying capacity of the strengthened slab depends on the effective strain of the CFRP. The tensile strain in the CFRP sheet was thus calculated for each load step until it reached the ultimate strain value, set at 0.017. Finally, the CQ48I element was used to simulate the adhesion between two planes with a zero thickness, specifically between the CFRP sheet and the concrete. The bond strength between CFRP and concrete was modeled by applying a shear stress (τ) versus slip (S) relationship, as proposed by Lu et al. [8], illustrated in Figure 1(d).

A validation of the NLFE models was realized by

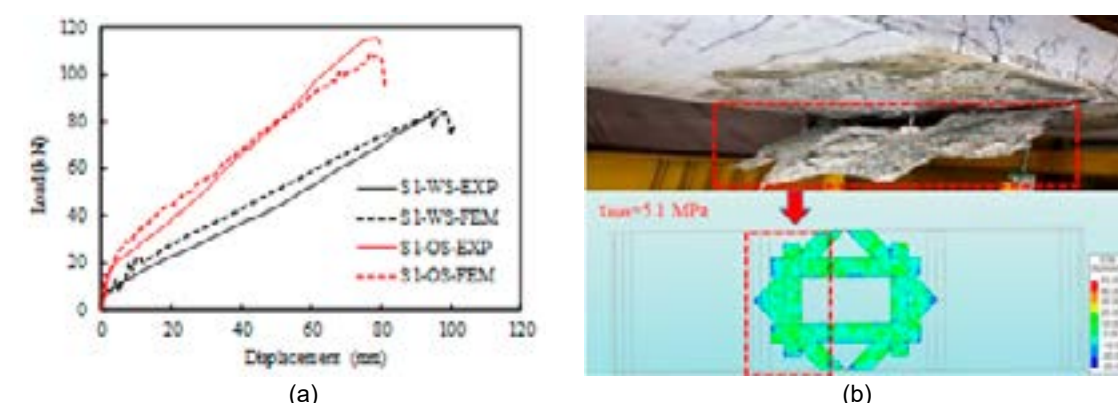


Figure 2. Comparison of experimental and numerical results: (a) Load-displacement curves and (b) failure mode

⁽¹⁾ Assoc. Prof. Dr., Hanoi University of Civil Engineering, E-mail: tannn@huce.edu.vn, sdt0387125125

⁽²⁾ Dr., Hanoi University of Civil Engineering, Email: tranadung101@gmail.com

⁽³⁾ Master student, Hanoi University of Civil Engineering, Email: trong230601@huce.edu.vn

comparing it with an experimental slab with a similar setup. The validation was realized for non-strengthened and strengthened slabs. The load was applied by increasing the displacement of two loading points spaced 1000 mm apart. The difference between experimental and numerical maximum loads, as in Figure 2(a), was less than 6.7% for the non-strengthened one (S1-WS), while for the strengthened one (S1-OS) was less than 6.9%. Furthermore, a comparison of the failure mode of the CFRP-strengthened slab from the experiment (EXP) and FEA was illustrated in Figure 2(b). This similarity allowed the use of the NLFE model for further investigation of the slab's behavior under parametric studies.

Table 1. Summary of experimental and numerical results

Slab notation	Maximum load (kN)		Displacement (mm)		$P_{u,FEA}/P_{u,EXP}$
	$P_{u,EXP}$	$P_{u,FEA}$	EXP	FEA	
S1-WS	90	84	93	94	0.933
S1-OS	116	108	79	79	0.931

3. Parametric study on the influencing factors

The above validation confirmed the similarity between the experiment and FEA. Thus, it is comprehensive to realize a parametric study on different factors that influence the performance of the CFRP-strengthened slabs with openings. This study helps better understand each of these factors and eventually maximize their use.

3.1. Compressive strength of concrete

In this section, four strengthened slabs were developed from the validated model S1-OS-FEM (with C35 concrete strength grade) to assess the influence of the compressive strengths of concrete. These modeled slabs, designated as S1-OS-C25, S1-OS-C30, S1-OS-C40, and S1-OS-C45, had the same dimensions and reinforcement layout as the S1-OS-FEM slab, with compressive strengths ranging from 25 MPa to 45 MPa. The maximum bond strength between FRP (e.g., CFRP sheets, GFRP bars) and concrete was also modified according to the compressive strength.

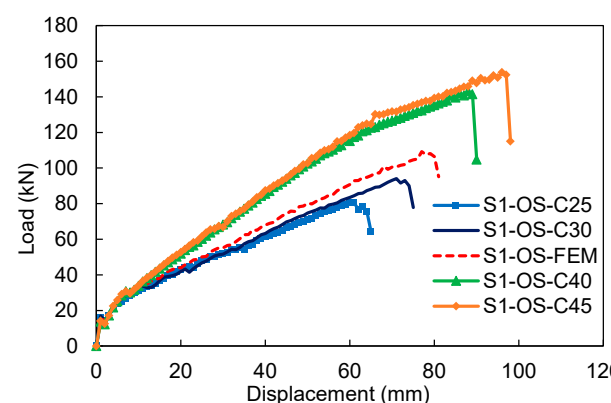


Figure 3. Load-displacement curves of CFRP-strengthened slabs with various compressive strengths of concrete

Conversely, increasing the concrete strength from C35 to higher strength significantly increased the maximum load capacity of the slab. With slab S1-OS-C40, a 32.3% increase in maximum load capacity (143 kN versus 108 kN) and an 11.4% increase in maximum displacement (88 mm versus 79 mm) were obtained, while with slab S1-OS-C45, these values were 39.1% (151 kN versus 108 kN) and 15.2% (91 mm versus 79 mm), respectively. The CFRP sheets on the last sample ruptured due to exceeding their permissible stress, and the slab continued to perform without them. It is evident that selecting the appropriate concrete compressive strength is crucial for the workability of a GFRP-reinforced concrete slab with openings strengthened with CFRP sheets.

3.2. GFRP reinforcement ratio
In this section, four strengthened slabs were developed from the validated model S1-OS-FEM to assess the effect of the GFRP reinforcement ratio. These modeled slabs were all made of concrete with a mean compressive strength of 49.2 MPa. The mechanical properties of GFRP bars were input to be equal between these samples. The only difference was the diameter of the GFRP bars in the tension zone of the slab, which varied from 8 mm to 6 mm, 10 mm, 12 mm, and 14 mm, while the spacing between the bars remained unchanged. They were designated as S1-OS-D6, S1-OS-D10, S1-OS-D12, and S1-OS-D14 respectively.

Figure 3 presents the load-displacement curves obtained from numerical results. It showed that reducing the concrete strength from C35 to C30 and C25 decreased the maximum load capacity of the slab by 13.1% and 25.5% (94 kN and 81 kN versus 108 kN), respectively. Additionally, their maximum displacement decreased from 79 mm to 71 mm with C30 concrete and 60 mm with C25 concrete. For these two samples, the CFRP sheets did not experience debonding at the maximum load capacity of the slab.

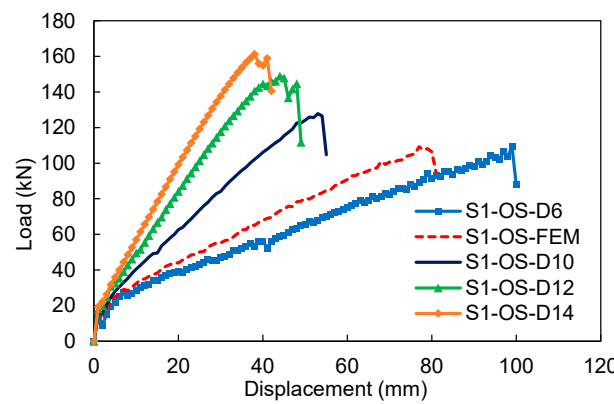


Figure 4. Load-displacement curves of CFRP-strengthened slabs with various GFRP reinforcement ratios

The load-displacement curves obtained from FEA were presented in Figure 4 for five modeled slabs. The maximum load capacity of the slab changed significantly when the diameter of the GFRP bars was decreased from 8 mm to 6 mm, while the maximum displacement increased by 25.3%. This highlights the impact of the GFRP reinforcement ratio on the ductility of the slab. In contrast, increasing the GFRP bar diameter from 8 mm to 10 mm resulted in an 18.1% increase in maximum load capacity (128 kN versus 108 kN). However, the maximum displacement was equal to 53 mm, which decreased by 32.9% compared to the reference sample. A similar trend was observed on slabs S1-OS-D12 with a maximum load of 149 kN at 44 mm displacement and S1-OS-D14 with a maximum load of 161 kN at 38 mm displacement. It can be observed that increasing the reinforcement ratio significantly reduces ductility (up to 59.1%) while increasing the ultimate strength of the slab sample (up to 49.1%). The result obtained from GFRP bars was similar to steel bars in structural components found by Mansor et al. [9].

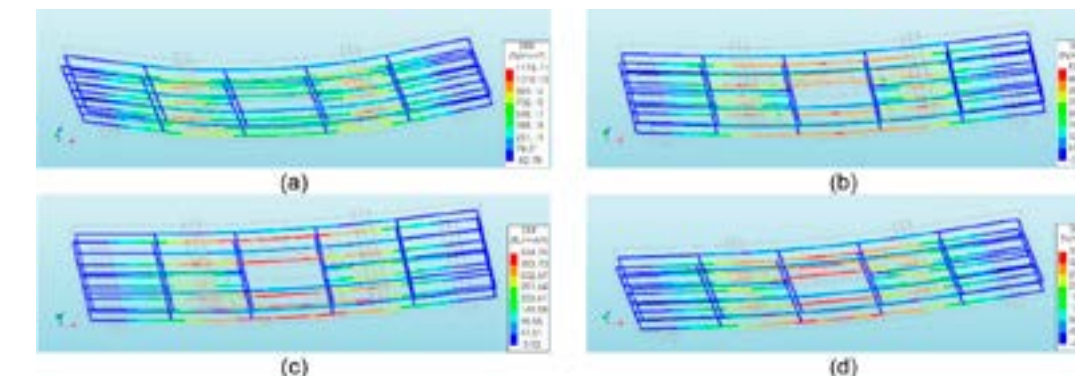


Figure 5. Stress distribution in GFRP bars at the maximum load: (a) S1-OS-D6, (b) S1-OS-D10, (c) S1-OS-D12, and (d) S1-OS-D14

The FEA results also provide insight into the stress distribution in GFRP reinforcement at a target applied load, such as the maximum load. Figure 5 shows the stress distribution in GFRP bars at the maximum load for four samples. The f_u value of GFRP bars was 1500 MPa (or 1500 N/mm²). Notably, as the diameter of the GFRP bars increased, their maximum stress values decreased, ranging from 1173.1 MPa in the D6 sample to 374.5 MPa in the D14 sample. This indicated that smaller GFRP bars experienced higher stress under the applied load. Additionally, the increased ductility of these samples allowed for greater beam deflection.

3.3. Disposition layout of CFRP sheets

In this section, three strengthened slabs were developed from the validated model S1-OS-FEM to assess the effect of the CFRP bonding layout. These modeled slabs, named S1-OS-L1, S1-OS-DC2, and S1-OS-L3, used a similar area of CFRP sheets equal to 0.5 m² but with different bonding layouts, as illustrated in Figure 6. Slab S1-OS-L1 was strengthened with a single layer of CFRP sheets having a smaller width and higher length. Slab S1-OS-L2 also used a single layer of CFRP sheets with a larger width and shorter length. Meanwhile, slab S1-OS-L3 was strengthened with two layers with a similar width as slab S1-OS-L1. A comparison of load-displacement curves of modeled slabs with slab S1-OS-FEM by FEA result was shown in Figure 7.

Changes in the reinforcement layouts significantly affected the load-carrying capacity of the slab. With a consistent CFRP area of 0.5 m², three different strengthening

layouts were simulated to evaluate their efficiency in terms of load-carrying performance and efficiency. The layout using two layers of 100 mm wide CFRP sheets, as shown in Figure 6(d), resulted in a slight change in maximum load capacity but a 12.7% reduction in maximum displacement. This was due to increased stiffness and reduced ductility, similar to the result in Figure 2(a). For the S1-OS-L1 sample with a single layer of 100 mm wide CFRP sheets, as shown in Figure 6(b), its maximum load capacity increased by 10.2% compared to slab S1-OS-FEM (119 kN versus 108 kN), but the maximum displacement decreased by 5.1% (75 mm versus 79 mm). This was due to stress exceeding the permissible limit in the CFRP sheets, which led to their rupture.

The analysis results indicated that the strengthening layout S1-OS-L2 was the most optimal. This layout, as illustrated in Figure 6(c), achieved a maximum load of 130 kN, corresponding to an increase of 20.1% compared to slab S1-OS-FEM, as illustrated in Figure 6(a). Furthermore, it presented an 11.4% increase in maximum displacement. This result showed that this layout increased the slab's stiffness without losing its ductility. The above results help to derive the influence of CFRP sheets' length and width on the performance of the slabs. The higher the length of CFRP sheets, the better the performance of the slabs. It was noted that the length of CFRP should be greater than a critical value (i.e., half of the slab's clear span). However, with a similar area of CFRP sheets, it would lead to a reduction in their width, which would lead to early failure.

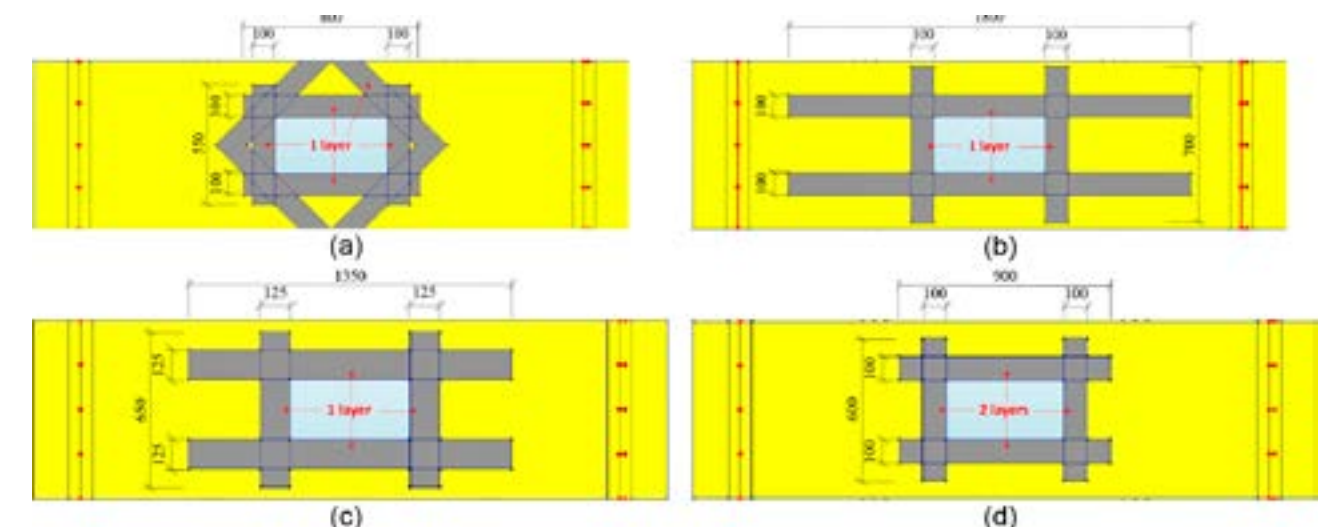


Figure 6. Illustration of CFRP strengthening layouts: (a) S1-OS-FEM, (b) S1-OS-L1, (c) S1-OS-L2, (d) S1-OS-L3

due to CFRP debonding. Therefore, it was recommended that the dimensions (i.e., length and width) and layout of the CFRP sheets be carefully considered to obtain the highest strengthening performance.

4. Conclusions

This research investigated the flexural behavior of one-way concrete slabs with openings reinforced with GFRP bars and strengthened using CFRP sheets through NLFE analysis. First, the results suggested that using proper concrete compressive strengths improved the performance of the slab, with better incorporation of CFRP sheets. In this study, the concrete compressive strengths ranging from 30 MPa to 35 MPa were more suitable with the sample's setup. Secondly, it can be observed that increasing the reinforcement ratio reduces ductility while increasing the ultimate strength of the slab sample. The GFRP bars also participated more in the case of a smaller reinforcement ratio. Finally, the disposition layout of CFRP sheets was considered, revealing its influence on the slab's stiffness and ductility. A disposition layout concentrated around

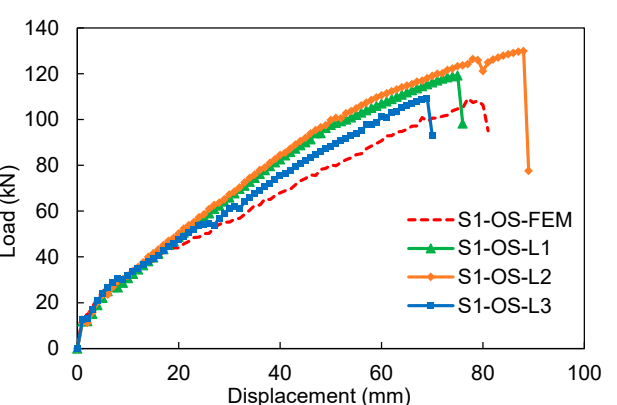


Figure 7. Load-displacement curves of CFRP-strengthened slabs with considered strengthening layouts

the opening improved its performance. The parametric investigations thus provided valuable insights into optimizing the structural performance of the considered slabs./.

References

1. M. Z. Naser, R. A. Hawileh, and J. A. Abdalla. Fiber-reinforced polymer composites in strengthening reinforced concrete structures: A critical review. *Engineering Structures*, vol. 198, 109542, 2019.
2. N. T. Nguyen, T. K. Nguyen, D. H. Du, D. N. Nguyen, and T. S. Kieu. Nonlinear finite element analysis of FRP-strengthened full-size reinforced concrete beams. *Innovative Infrastructure Solutions*, vol. 8, no. 5, p. 139, 2023.
3. Ö. Anil, N. Kaya, and O. Arslan. Strengthening of one-way RC slab with opening using CFRP strips. *Construction and Building Materials*, vol. 48, 883–893, 2013.
4. H. M. Afefy and T. M. Fawzy. Strengthening of RC one-way slabs including cut-out using different techniques. *Engineering Structures*, vol. 57, 23–36, 2013.
5. T. K. Nguyen, N. T. Nguyen, H. A. Tran, H. G. Nguyen, and P. Tran. Three-dimensional nonlinear finite element analysis of corroded reinforced concrete beams strengthened by CFRP sheets. *European Journal of Environmental and Civil Engineering*, 1–27, 2024.
6. H. D. Vu and D. N. Phan. A framework for predicting the debonding failure modes of RC beams strengthened flexurally with FRP sheets. *Innovative Infrastructure Solutions*, vol. 7, no. 5, 292, 2022.
7. M. A. Golham and A. H. A. Al-Ahmed. Strengthening of GFRP Reinforced Concrete Slabs with Openings. *Journal of Engineering*, vol. 30, no. 01, 157–172, 2024.
8. X. Z. Lu, J. G. Teng, L. P. Ye, and J. J. Jiang. Bond-slip models for FRP sheets/plates bonded to concrete. *Engineering Structures*, vol. 27, no. 6, 920–937, 2005.
9. A. A. Mansor, A. S. Mohammed, and W. D. Salman. Effect of longitudinal steel reinforcement ratio on deflection and ductility in reinforced concrete beams. *IOP Conference Series: Materials Science and Engineering*, vol. 888, no. 1, 012008, Jul. 2020.

Reflection, transmission of QP-wave at an imperfect interface...

(tiếp theo trang 37)

the reflection coefficients of waves in an imperfect interface are greater than the ones in slip interface while transmission coefficients are the opposite. For the case of slip interface, the valley value of the reflection coefficient of QP wave is attained at $\theta_0=24^\circ$; 24° , while that one is attained at $\theta_0=68^\circ$; 72° for imperfect interface.

6. Conclusion

In conclusion, a mathematical study of reflection

and transmission coefficients at an imperfect interface separating two transversely isotropic nonlocal elastic solid half spaces is made when longitudinal wave is incident. The three cases of imperfect interfaces are discussed briefly. For the incidence QP wave, the expressions for reflection, transmission coefficients of waves in the imperfect/perfect cases are given. Numerical computations have been performed for a particular model and the results obtained are depicted graphically./.

References

1. Z. Hashin, The spherical inclusion with imperfect interface. *J. Appl. Mech.*, vol. 58, no. 2, pp. 444–449, 1991.
2. S. I. Rokhlin and Y. J. Wang, Analysis of boundary conditions for elastic wave interaction with an interface between two solids. *J. Acoust. Soc. Am.*, vol. 89, no. 2, pp. 503–515, 1991.
3. J. D. Achenbach, *Wave Propagation in Elastic Solids*. vol. 16. Series in Applied Mechanics. North Holland: Amsterdam. 1973
4. A. H. Nayfeh, *Wave Propagation in Layered Anisotropic Media*, North-Holland: Amsterdam, 1995.
5. D. X. Tung, The reflection and transmission of waves at an imperfect interface between two nonlocal transversely isotropic liquid-saturated porous half spaces. *Waves Random Complex Media*, pp. 1–17, 2021.
6. S. Goyal, S. Sahu and S. Mondal, Influence of imperfect bonding on the reflection and transmission of QP-wave at the interface of two functionally graded piezoelectric materials. *Wave Motion*, vol. 92, pp. 102431, 2020.

Some safety issues in construction of climbing formwork system in high - rise building construction in Vietnam

Trinh Xuan Vinh⁽¹⁾, Tran Tien Huynh⁽²⁾

Abstract

The paper presents some safety issues in the construction of climbing formwork systems in high-rise building construction in Vietnam.

High-rise buildings impose stringent safety requirements on the implementation of climbing formwork systems. A specific safety plan must be in place, including identifying and eliminating potential hazards, providing adequate personal protective equipment, and ensuring compliance with industry safety regulations and standards.

Safety practices in Vietnam adhere to the national technical standard QCVN 18:2021/BXD on Safety in Construction and draw from international organizations such as OSHA (Occupational Safety and Health Administration of the United States), CEN (European Committee for Standardization), and Japan's guidelines on construction safety regulations. These references provide specific guidance and international standards for the construction of climbing formwork systems.

Key words: Safety; climbing formwork systems; high-rise building



Figure 1. The Landmark81, Ho Chi Minh City. Source: <https://www.coteccons.vn>

2. Safety Requirement

High-rise buildings impose stringent safety requirements on the implementation of climbing formwork systems. A specific safety plan must be in place, including identifying and eliminating potential hazards, providing adequate personal protective equipment, and ensuring compliance with industry safety regulations and standards.

Safety practices in Vietnam adhere to the national technical standard QCVN 18:2021/BXD on Safety in Construction and draw from international organizations such as OSHA (Occupational Safety and Health Administration of the United States), CEN (European Committee for Standardization), and Japan's guidelines on construction safety regulations. These references provide specific guidance and international standards for the construction of climbing formwork systems.

In recent years, climbing formwork systems have been widely used in Vietnam due to their ability to meet project schedules, quality requirements, and especially high levels of occupational safety. Safety measures for climbing formwork systems require strict adherence throughout the installation and dismantling processes.

For installation work, the following requirements apply:

- Large formwork panels for multiple levels should only be installed after the formwork for lower levels has been securely fixed.